APOLLO SPACECRAFT SOFTWARE CONFIGURATION CONTROL BOARD PROGRAM CHANGE REQUEST

NUMBER (Completed by FSB): 890

1.0 COMPLETED BY ORIGINATOR

1.1 ORIGINATOR	DATE	1.2 ORGANIZATION	APPROVAL	DATE
G. R. Kalan	8/14/69	MIT/IL	George W. Cherry	8/18/69

1.3 EFFECTIVITY	1.4 TITLE OF CHANGE
LUMINARY II	Improve slosh stability of CSM - docked DAP

1.5 REASON(S) FOR CHANGE

See Data Amplification Sheet

1.6 DESCRIPTION OF CHANGE

Modify rate and acceleration gains and, if necessary, trap size in CSM-docked state estimator.

2.0 SOFTWARE CONTROL BOARD OR FLIGHT SOFTWARE BRANCH DECISION FOR VISIBILITY IMPACT ESTIMATE BY MIT

2.1 ☐ APPROVED ☐ DISAPPROVED

2.2 REMARKS:

2.3 SOFTWARE CONTROL BOARD OR FLIGHT SOFTWARE BRANCH SIGN OFF

DATE

3.0 MIT VISIBILITY IMPACT EVALUATION:

3.1 SCHEDULE IMPACT

3.2 IMPACT OF PROVIDING DETAILED EVALUATION

3.3 STORAGE IMPACT

0

3.4 REMARKS:

3.5 MIT COORDINATOR

DATE

4.0 SOFTWARE CONTROL BOARD ACTION

4.1 ☐ IMPLEMENT AND PROVIDE DETAILED CHANGE EVAL. ☒ PROVIDE DETAILED CHANGE EVALUATION ☐ DIS-APPROVED

4.2 REMARKS

Approved for off line assembly

4.3 SOFTWARE CONTROL BOARD SIGN OFF

[signature]

DATE

10-9-69

5.0 MIT DETAILED PROGRAM CHANGE EVALUATION

5.1 MIT COORDINATOR

DATE

5.2 MIT EVALUATION

6.0 SOFTWARE CONTROL BOARD DECISION ON MIT DETAILED PROGRAM CHANGE EVALUATION

6.1 ☐ START OR CONTINUE IMPLEMENTATION ☐ DISAPPROVED OR STOP IMPLEMENTATION

6.2 REMARKS:

6.3 SOFTWARE CONTROL BOARD SIGN OFF

DATE

APOLLO SPACECRAFT SOFTWARE CONFIGURATION CONTROL BOARD

-DATA AMPLIFICATION SHEET -

PROGRAM CHANGE REQUEST NO. 890	PREPARED BY: G. R. Kalan DATE: 8/14/69	ORGANIZATION: MIT/IL

CONTINUATION SECTION (REFER TO BLOCK NUMBER AND TITLE ON PROGRAM CHANGE REQUEST FORM)

1.5 Reason For Change:

Due to various hardware and software lags, the GTS attitude control system pumps energy into the slosh oscillation modes in the CSM-docked configuration. A significant portion of the software lag is caused by the large time constants of the CSM-docked state estimator. Although the low gain state estimator was necessary in the SUNDANCE and LUMINARY 1 DAPS to prevent bending mode instabilities, the improvement in bending stability with the jet inhibition logic introduced in LUMINARY 1A should be sufficient to allow the use of a faster state estimator.

REMARKS

TP#2181

NASA — MSC — Coml., Houston, Texas

Massachusetts Institute of Technology
Instrumentation Laboratory
Cambridge, Massachusetts

Spacecraft Autopilot Development Memo #30-69

TO: Distribution

FROM: Craig Work

DATE: 30 September 1969

SUBJECT: LUMINARY 1A: CSM-DOCKED LM DAP MISSION F SLOSH STABILITY

Recent communications from NASA and TRW have added urgency to the investigation of possible slosh-guidance-control interactions in the LGC program LUMINARY. (See reference 1.)

Our previous investigations have established that CSM-docked trim gimbal control, as exercised by the LM digital autopilot in the earlier program SUNDANCE, was almost neutrally stable with respect to slosh; that is very little energy was added to or extracted from the slosh modes. Similar tests on LUMINARY showed that energy was being pumped into the slosh process by the DAP, and in particular by the attitude control mode of the GTS. This report summarizes the results of initial efforts to a) analyze the CSM-docked DAP response to slosh, b) determine what DAP responses would be desirable, c) predict the results of various possible DAP changes, d) implement and test appropriate DAP changes.

The interactive feed-back between the DAP state-estimator (SE) and the GTS lead to an approach in which the SE-GTS combination was treated as a single operator, accepting sensor information, a previous state estimate, and guidance commands as input and producing trim gimbal drive commands and a modified state estimate as output.

DAP response to a pure unvarying harmonic input was the first body of information to be sought, both because linear control theory provides useful interpretations for such information and because real slosh inputs to the DAP take just that form. In order to fulfill part

a) of the given set of goals, it was necessary to determine a range of slosh parameter values over which the DAP response should be analyzed. Taking the slosh input as having the form $\theta = A \sin (2\pi ft)$, where A is slosh amplitude and f is the frequency of the oscillation, range determinations were needed for A and f. The environmental slosh model was examined in order to establish those ranges.

In the MIT-IL Apollo environment simulation, the effect of propellant sloshing in the LM tanks is modeled as a two-dimensional mass-spring oscillator for each propellant tank; RCS tanks are neglected (see reference 2). The slosh frequency is given by ω,

$$\omega = \lambda (\alpha_x/R)^{1/2} \quad (1)$$

where λ is calculated for CSM model, but for LM, it is a tabulated function of the liquid level in the tank,

α_x is the contact acceleration along the vehicle X axis, and

R is the radius of the tank in question.

The slosh mass force is then described by

$$F_s = -kx_s \quad (2)$$

where x_s is the slosh mass horizontal displacement from the slosh mass attachment point,

k is a parameter, the "spring contant".

If the slosh mass is assumed to be constant during an interval under discussion, $x_s = (-k/M_s)x_s$ (3)

where x_s is the second time derivative of x_s,

M_s is the slosh mass for the designated tank.

Solving Eq (3) for x_s yields a harmonic form with the frequency ω determined as

$$\omega = (k/M_s)^{1/2}, \quad (4)$$

where ω is the same in Eqs (1) and (4)

Equation (1) was used to determine values for ω, which are tabulated below in Table 1.

TABLE 1. High Thrust CSM-docked LM Slosh Frequencies

	Fuel Tanks	Frequencies
Heaviest Vehicle	APS	0.465 cps
	DPS	0.497 cps
	CSM	0.580 cps
Lightest Vehicle	APS	0.338 cps
	DPS	0.333 cps
	CSM	0.388 cps

Equation (4) shows $\omega^2 = k/M_s$. But

$$F_v = -Kx_v \tag{5}$$

describes the "equal and opposite force" applied to the vehicle, where

x_v = vehicle displacement from rest position,

K = vehicle "spring constant,"

and the sign of x_s opposes that of x_v. Assuming the vehicle mass to change only negligibly in a limited time period,

$$\ddot{x}_v = (-K/M_v)x_v \tag{6}$$

as in eq (3), where

$\ddot{x}_v$ is the second time derivative of x_v,

M_v is the total vehicle mass, excluding the slosh mass.

Solving eq (6) yields

$$\omega^2 = K/M_v \tag{7}$$

and we can then say that, since the force is of the same magnitude in equations (5) and (2), and since

ω is the same in equations (7) and (4),

$$K = \frac{M_v k}{M_s} \quad \text{and} \tag{8}$$

$$x_v = \frac{M_s k}{M_v} x_s . \quad (9)$$

Equation (9) provides a start in estimating the total displacement, x_v, for the vehicle. Taking a worst case, in which each tank has its maximum slosh mass, and all tanks are in phase with indentical frequencies, oscillating to the maximum amplitudes, an extreme maximum horizontal vehicle displacement can be found. Dividing this by the radius of gyration computed for the combined slosh masses yields a good value for the tangent of the angle subtended at the vehicle center of mass by the vehicle rotation from the zero position in worst case slosh. Maximum slosh masses and radial distances were obtained from references 3, 4 and 5, yielding a radius of gyration of 4.14 meters. M_s = 2451 kg and $M_s + M_v$ = 31615 kg describe maximum slosh mass and total mass appropriate to an emergency CSM-docked DPS LM-active TEI burn. Using a representative tank radius of 0.65 meters for x_s max, we get

$$x_v \text{ max} = 0.0546 \text{ meters} \quad (10)$$

$$\arctan (0.0546/4.14) = 0.756^\circ \text{ as the} \quad (11)$$

worst case angular displacement amplitude. A value for this amplitude, determined by a conservation of momentum argument, was found to be in close agreement. A matrix of three frequencies $f = \omega/2\pi$ and three amplitudes A was tested as follows. Digital simulations were run in which

a) The LGC ignored the true CDUs and used some dummy CDU cells instead.

b) The dummy CDU cells provided zeroes for CDUX, CDUY, and provided $\theta = A \sin (2\pi ft)$ for CDUZ, with the desired (CDUD) values zeroed.

c) The mass monitor was turned off, so that mass was not decremented.

d) The RCS jet commands were not implemented nor were the GTS commands. The State Estimator information feedback from RCS and GTS included the RCS non-activity but ignored the GTS non-activity. This was intended to display the CSM-docked DAP response to a steady-state situation in which slosh oscillations were present.

In order to evaluate the results of these runs, it was noted that slosh energy-draining ideal GTS drives should induce angular accelerations which would always oppose the sign of the true slosh-induced angular velocity. Therefore, the GTS drive pattern frequency would match the frequency f of $\theta = A \sin(2\pi ft)$. The derivative of the GTS-induced angular accelerations is the square-wave plot of the drives themselves, and the square-wave leads the acceleration curve by one-quarter cycle, or 90°. The true angular velocity is not available in the State Estimator, but it is the derivative of the raw input θ, and must lead θ by one-quarter cycle, or 90°. Therefore, if GTS-induced angular acceleration and input rate are to be exactly opposed to one another, then the GTS drives and the input θ must agree exactly in sign; they must have the same period and phase. This criterion enables us to evaluate the CSM-docked DAP performance, keeping in mind that the GTS drives are normally implemented 0.18 seconds after they are determined, in the LUMINARY CSM-docked DAP. Accordingly, ideal slosh-draining GTS drive computations will agree in period and phase with $\theta^* = A \sin(2\pi f(t + 0.18))$.

The matrix of tests was run, and the results are summarized in Table 2 and Figures 1, 2, and 3. Earlier observations and experience were confirmed when these tests showed the State-Estimator-GTS combination to be producing almost perfect slosh-<u>pumping</u> drives for the range of frequencies and amplitudes being examined.

TABLE 2

Cell entries: GTS θ^* % sign agreement
GTS phase lag
GTS delay time

	A = 0.8°	A = 0.5°	A = 0.2°
f = 0.6 cps	17.1% 211.8° 0.981 sec	15.6% 208.1° 0.964 sec	21.1% 218.2° 1.010 sec
f = 0.4 cps	6.47% 191.5° 1.330 sec	14.9% 207.0° 1.438 sec	11.0% 199.9° 1.388 sec
f = 0.26667 cps	1.78% 176.8° 1.84 sec	3.87% 172.3° 1.805 sec	6.55% 168.2° 1.752 sec

$$\theta^* = A \sin(2\pi f(t + 0.18))$$

Direct measurement of the dot product of the DPS engine torque vector and the slosh-induced angular velocity vector in normal digital simulations has also indicated the fact of slosh pumping, confirming the results of Table 2. Some values to hold in mind when scanning Table 2 cell entries are:

a) 100% GTS-θ^* agreement is perfect drain on slosh energy, 0% is perfect pumping, 50% is neutral stability.

b) 180° GTS phase lag is perfect pumping; while 90° or 270° represent neutral stability.

In accordance with parts c) and d) of the goals stated at the beginning of this report, solutions to this slosh-pumping problem are being determined and tested. The results of that effort will be reported when the project is complete.

References

No. 1: TRW, Interoffice Correspondence #69:7254.4-80, dated 13 May 1969, from W. R. Hamel to Task E-72A File, subject: "Docked DPS Slosh Instability for Mission F Contingency TEI Sequence".

No. 2: Guidance System Operations Plan, Section 6 Control Data, R-567, MIT-IL, November 1968, page 6-32.

No. 3: op. cit. page 6-33.

No. 4: op. cit. page 6-6.

No. 5: Guidance System Operations Plan, Section 6 Control Data, R-577, MIT-IL, December 1968, page 6-39, ff.

Distribution List

Internal

Group 23C
D. Hoag
R. Battin
L. Larson
N. Sears
G. Cherry
A. Klumpp
J. O'Connor
J. Dunbar
C. Work (2)

External

GAEC:	R. Portnoy H. Berman C. Tillman
NASA/MSC:	K. Cox W. Peters
TRW:	W.R. Hamel

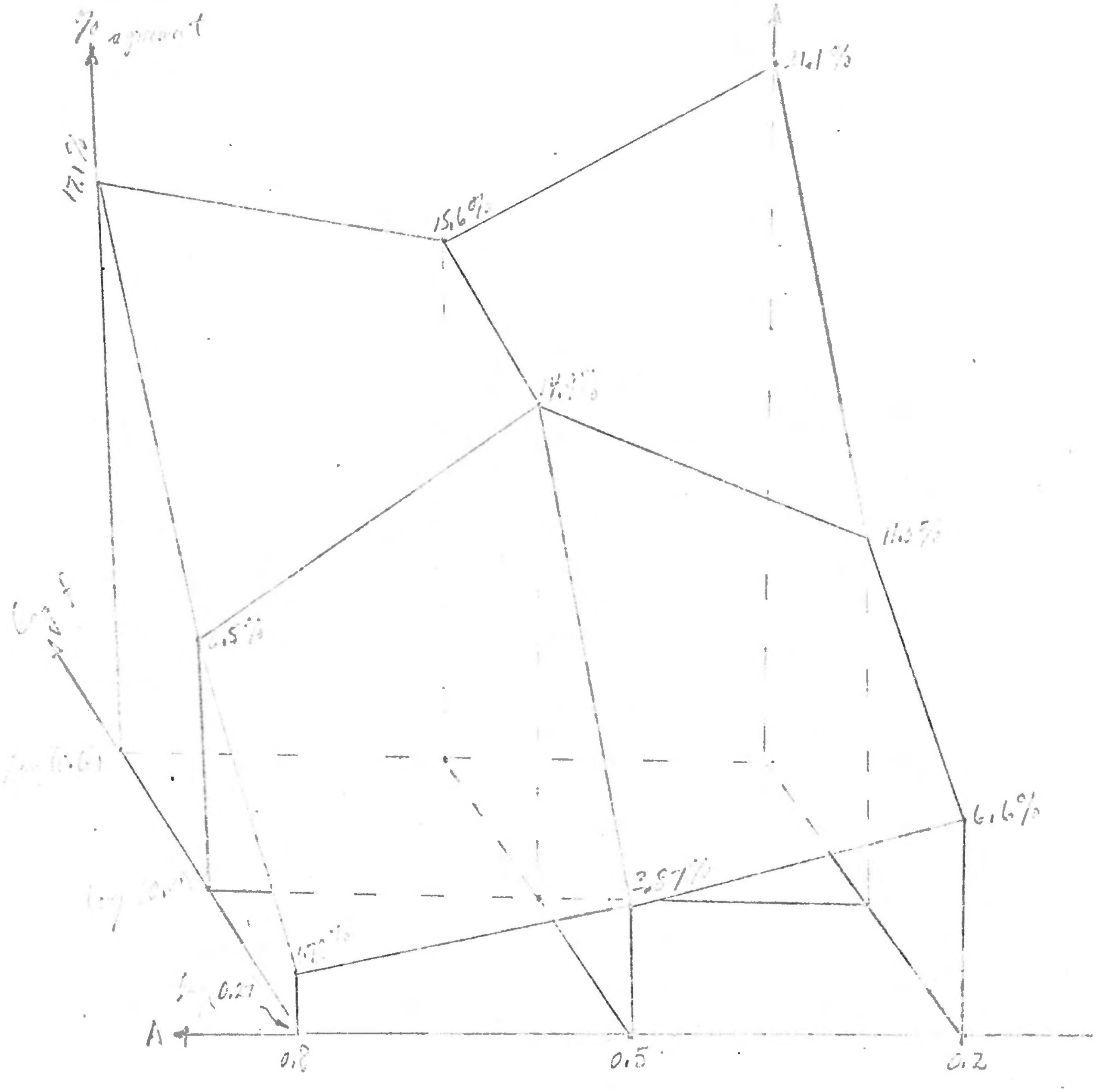

Figure 1. % Agreement of sgn(θ) and sgn(GTS), plotted against Amplitude (A) and log frequency (log f) of $\theta^* = A\sin(2\pi f(t+0.18))$.

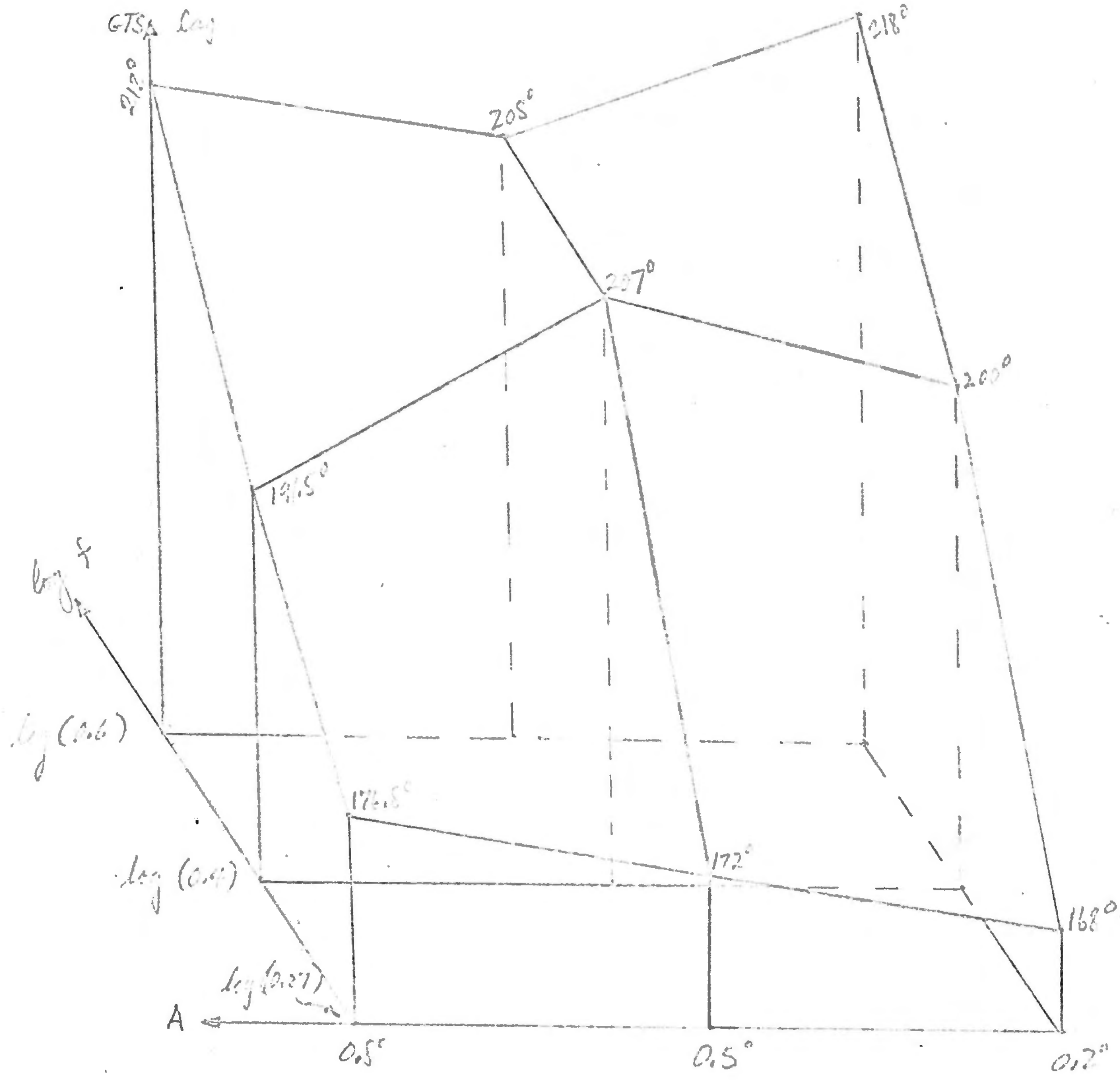

Figure 2. GTS phase lag behind $\theta^* = A\sin(2\pi f(t + 0.18))$ versus Amplitude (A) and log frequency (log f).

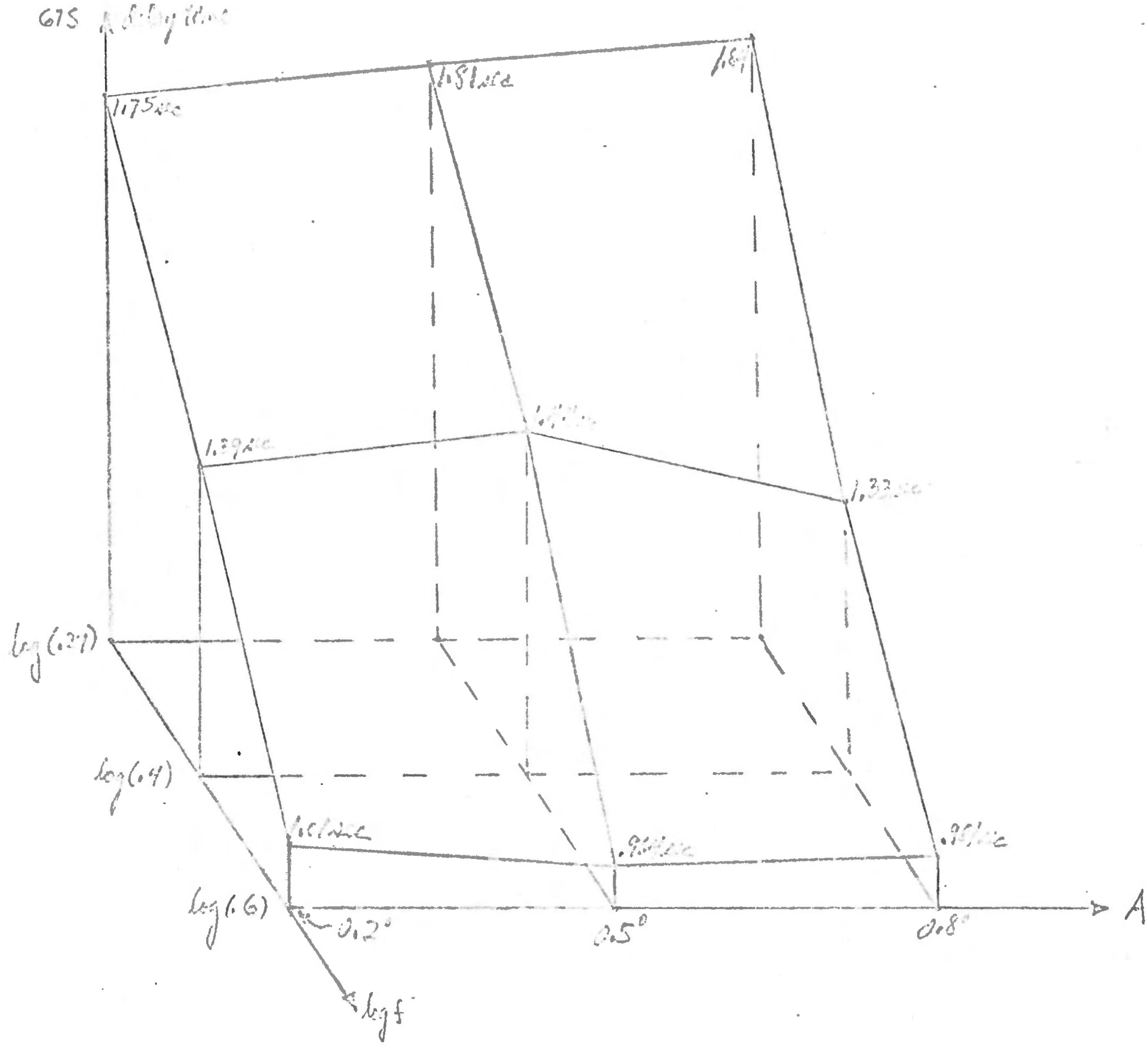

Figure 3. GTS delay time behind $\theta^* = A \sin(2\pi f(t + 0.18))$ versus Amplitude (A) and log frequency (log f).